Journal of Materials Chemistry B

Accepted Manuscript

ROYAL SOCIETY OF CHEMISTRY

www.rsc.org/materialsB

Cite this: DOI: 10.1039/c0xx00000x

www.rsc.org/xxxxxx

ARTICLE TYPE

Silica cross-linked nanoparticles encapsulating phenothiazine-derived Schiff base for selective detection of Fe (III) in aqueous media

Fangyuan Gai,[a] Xiang Li,[a] Tianlei Zhou,[b] Xiaogang Zhao,[c] Dongdong Lu,[a] Yunling Liu[a] and Qisheng Huo*[a]

Received (in XXX, XXX) Xth XXXXXXXXX 20XX, Accepted Xth XXXXXXXXX 20XX

DOI: 10.1039/b000000x

This work demonstrated that a luminescent chemosensor based on silica cross-linked micellar nanoparticles (SCMNPs) was design by encapsulating a phenothiazine-derived schiff base, (4E)-4-((10-dodecyl-10H-phenothiazin-7-yl) methyleneamino)-1,2-dihydro-1,5-dimethyl-2-phenylpyrazol-3-one (EDDP), for the selective detection of Fe^{3+}. The encapsulation of EDDP inside SCMNPs (EDDP-SCMNPs) can avoid the metal (Fe^{3+}/Fe^{2+})-promoted hydrolysis of EDDP and thus, exhibit a highly selective determination of Fe^{3+}. The electron transfer (ET) from EDDP in the core to Fe^{3+} adsorbed on the shell of EDDP-SCMNPs was verified by using UV-vis absorption, fluorescent emission and 3D fluorescence spectra. Moreover, EDDP-SCMNPs showed no sensing ability of Fe^{2+} due to the weak electron-accepting ability of Fe^{2+}. Significantly, because of the ultrasmall size, nontoxity, high water solubility and biocompatibility of EDDP-SCMNPs, this material has potential application in biological system.

Introduction

Iron is one of the most abundant essential elements in biological and environmental systems. [1, 2] Iron plays important role in living organisms for human health with the process of oxygen metabolism[3] and the intracellular chemical reactions catalysis.[3, 4] Its high oxygen affinity and facile redox chemistry facilitated the processes of electronic transfer to transport oxygen from the lungs to the tissues and diffuse oxygen in muscle cells.[5, 6] Although ferrous/ferric (Fe^{2+}/Fe^{3+}) states are the important redox pairs for the proper functioning of most living cells, both their deficiency and excess from the normal state limit may induces the occurrence of many serious diseases and disorders.[7-10] For example, Fe^{3+} overload and deficiency may cause severe tissue damage and organ dysfunction, which potentially interact with a number of health problems such as rectal cancer and iron deficiency anemia.[1, 9, 11-14] Therefore, biological systems need to keep a balance between Fe^{2+} and Fe^{3+} by regulate cellular iron homeostasis.

It is crucial to explore effective strategies for the determination of Fe^{2+}/Fe^{3+} selectively in many fields such as clinical, medical, environmental and also some industrial systems.[15, 16] A variety of traditional analytical techniques[17-21] have been used to detect Fe^{2+}/Fe^{3+}. Nevertheless, there are still limitations in biological system, such as the destruction of the samples and inconvenient of on-line monitoring.[22-24] As one of the effective method, optical imaging with fluorescence analysis of Fe^{2+}/Fe^{3+} has been developed most rapidly because of its high sensitivity, feasibility and throughout arrays.[25] The fluorescence sensing systems usually use organic chromophores[12, 26, 27] as light-emitting part which fluorescence changes act as a signal to indicate the presence of Fe^{2+}/Fe^{3+}. Most of organic chromophores were prepared by modification of rhodamine, benzothiazole and 8-hydroxyquinoline with functional groups to achieve photoinduced electron transfer (PET), fluorescence resonance energy transfer (FRET), excited state intramolecular proton transfer (ESIPT), twisted internal charge transfer (TICT) and so forth processes for iron sensing.[13, 28-33] Good selectivity and detection limit on Fe^{2+}/Fe^{3+} sensing have been successfully reached via above processes. However, the poor solubility in water and the biocompatibility of most sensing systems are still a challenge for *in vivo* sensing.

To determine Fe^{3+}/Fe^{2+} in the living system, a need for water soluble luminescent chemosensor with good biocompatibility and nontoxity is growing. Multicomponent systems[34-38] incorporating with both organic chromophores and inorganic scaffolds have been proposed to construct a suitable way for meeting these requirements.[32, 39, 40] For example, Zhang *et al.* have prepared graphene oxide (GO) nanosheet which functionalized with organic moieties to achieve highly selective detection of Fe^{3+} in living cell.[41] This method also can be used for the detection of Fe^{2+} via an oxidation process using H_2O_2. [41, 42] Although few systems have been built for the selective sensing of Fe^{3+},[7, 41, 43] the inorganic scaffolds of multicomponent sensing system still meets challenges including dispersity and nanosize in the biological application.

Recently, silica cross-linked micellar nanoparticles (SCMNPs) have been introduced into multicomponent system as a inorganic scaffold to construct various ion sensor and chemical sensor for pH, Cu, etc. [28, 44, 45] In these sensing systems, optical properties of organic dyes were protected by SCMNPs with nanosize of ~15nm and with good dispersity in aqueous media. Our previous work has reported SCMNPs-based fluorescence imaging system via a energy transfer process for signal amplification of TPP sensing.[46]

In this paper, we have encapsulated a phenothiazine-derived schiff base, (4E)-4-((10-dodecyl-10H-phenothiazin-7-yl) methyleneamino)-1,2-dihydro-1,5-dimethyl-2-phenylpyrazol-3-one (EDDP), in SCMNPs to build water-soluble luminescence nanoparticles, EDDP-SCMNPs, for highly selective determination of Fe^{3+} from other common cations including Fe^{2+} in aqueous media. EDDP-SCMNPs can easily adsorb Fe^{3+} onto its shell and protect EDDP from being metal-promoted hydrolysis. Moreover, the distances between EDDP molecules and Fe^{3+} ions on shell is close enough to quench EDDP-SCMNPs fluorescence through electron transfer (ET) process.

Experimental section

Materials

Pluronic nonionic surfactant F127, diethoxydimethylsilane ($Me_2Si(OEt)_2$, DEDMS) and tetraethylorthosilicate (TEOS, 99.99%) were purchased from Sigma-Adrich. Ethanol(CH_3CH_2OH, 95%), Acetic acid (CH_3COOH, ≥99.5 %), Ferrous chloride tetrahydrate ($FeCl_2\cdot 4H_2O$, 99%), phenothiazine (≥98%), hydrochloric acid (HCl, ≥37%), anhydrous ferric chloride ($FeCl_3$, ≥97%), acetonitrile (CH_3CN, ≥97 %), and sodium hydride (NaH, 60%) were purchased from Aladdin. 4-Aminoantipyrine (98%) was purchased from Alfa Aesar. The dialysis tubing (M_w cutoff: 8,000-14,400) was purchased from Aldrich. All reagents and solvents were used without further purification. Deionised water was used in our experiment (resistivity ≥ 18.2 MΩ).

Synthesis of EDDP

The synthetic detail of EDDP ((4E)-4-((10-dodecyl-10H-phenothiazin-7-yl) methyleneamino)-1, 2-dihydro-1,5-dimethyl-2-phenylpyrazol-3-one) was shown in the supporting information. First, 10-dodecyl-10H-phenothiazine was synthesised according to literature (Scheme S1).[47] 10-dodecyl-10H-phenothiazine-3-carbaldehyde was obtained via a Vilsmeier reaction. Phenothiazine-derived Schiff base, (4E)-4-((10-dodecyl-10H-phenothiazin-7-yl) methyleneamino)-1,2-dihydro-1,5-dimethyl-2-phenylpyrazol-3-one (EDDP), was prepared as a yellow precipitate from the mixture of ethanol, acetic acid, 10-dodecyl-10H-phenothiazine-3-carbaldehyde, and 4-aminoantipyrine under reflux for 3h. The ^{1}H NMR data of synthesized EDDP was shown in the Fig. S1.

Synthesis of the EDDP-SCMNPs

First, an acidic aqueous solution of F127 (0.6 g of F127 in 9.4 g of 0.85 M HCl solution) was added to a glass vial. 1 g of TEOS was added. After an additional 0.5 h of stirring, 0.06 g of DEDMS was then added. The as-made product was dialyzed against water to remove HCl and get silica cross-linked micellar nanoparticles (SCMNPs).[28, 39, 44-46] 0.1ml of the EDDP solution (10^{-4} M) in acetonitrile was put into a glass vial and then the solvents were completely removed in a vacuum oven at 40 □. Then, 2ml SCMNPs suspension was added in to the vial, and after 0.5 h of stirring, the EDDP-SCMNPs were treated with dialysis using a dialysis tube (cutoff: 8,000-14,400) and a 0.22 μm Teflon filter to ensure that all the low molecular (such as HCl and silane) and large solid impurities would be removed from the product.[45, 46]

Stability of EDDP-SCMNPs

The leakage of the EDDP from SCMNPs was tested using a dialysis method.[46] After a dialysis process for 1 h, the solutions inside and outside of the dialysis tube were both analyzed with inductively coupled plasma (ICP) for Si element and fluorescence emission spectrum for EDDP.

Characterization

Transmission electron microscopy (TEM) was carried out using FEI Tecnal G2 F20 s-twin D573 operated at 200 kV. The sample for TEM was prepared by directly placing a small drop of the nanoparticles suspension on a carbon-coated TEM grid. Measurements of UV absorption of the samples were done with a Perkin-Elmer Lambda 20 spectrometer. Inductively coupled plasma (ICP) analyses were carried out on a Perkin-Elmer Optima 3300DV ICP instrument. The particle size of SCMNPs was measured by a Malvern Zetasizer Nano-S instrument using Dynamic Light Scattering (DLS) principles with a HeNe laser (633 nm). The fluorescence emission spectra of the samples were recorded on an Edinburgh Instruments FLS920 spectrofluorimeter equipped with both continuous (450 W) and pulsed xenon lamps. ^{1}H NMR of EDDP were obtained on an Avance III instrument (Brucker, 300 MHz). Mass spectrometry (MS) of EDDP was carried out on a Brucker Instrument (Agilent1290-micrOTOF Q II).

Result and discussion

Our basic idea is to incorporate EDDP with SCMNPs for highly selective determination of Fe^{3+} via a electron transfer (ET) process[15, 41] instead of metal-promoted hydrolysis.[8] SCMNPs can prevent the fluorescence of EDDP from being quenched by the Fe^{3+}/Fe^{2+}-promoted hydrolysis. The structure and feature of EDDP-SCMNPs can result in the occurrence of electron transfer (ET) process from EDDP to Fe^{3+}. Therefore, we designed and synthesized EDDP-SCMNPs as a water-soluble fluorescence system for distinction between $Fe^{3+}$and Fe^{2+}.

Synthesis of EDDP-SCMNPs

EDDP was designed and synthesized to construct a schiff base derivative with D-π-A structure which can favour ET process from the core of SCMNPs. As is shown in Scheme 1, EDDP-SCMNPs were prepared via a simple encapsulation method.[28, 45, 46] After dialysis, stable EDDP-SCMNPs were obtained. The stability and monodispersion of EDDP-SCMNPs were similar to those for dye-SCMNPs reported in our previous work[46]. The fluorescence emission of EDDP-SCMNPs remains unchanged.

The features of EDDP-SCMNPs were investigated by DLS and TEM (See Fig. 1 and Fig. S2). The result of DLS shows the diameter of EDDP-SCMNPs was about 24nm with a narrow size distribution. The size of nanoaparticles based on TEM result (13nm) is accord with that reported in the literature.[45] The particle size based on DLS is larger than that from TEM. The reason is that the DLS data includes the contribution of PEO chains.[45, 48] EDDP-SCMNPs showed monodisperse morphology in TEM image which is ascribe to the extended PEO chains enable EDDP-SCMNPs dissolved in aqueous media. The size and morphology of EDDP-SCMNPs were similar to those of dye-SCMNPs in our previous work.[45, 46]

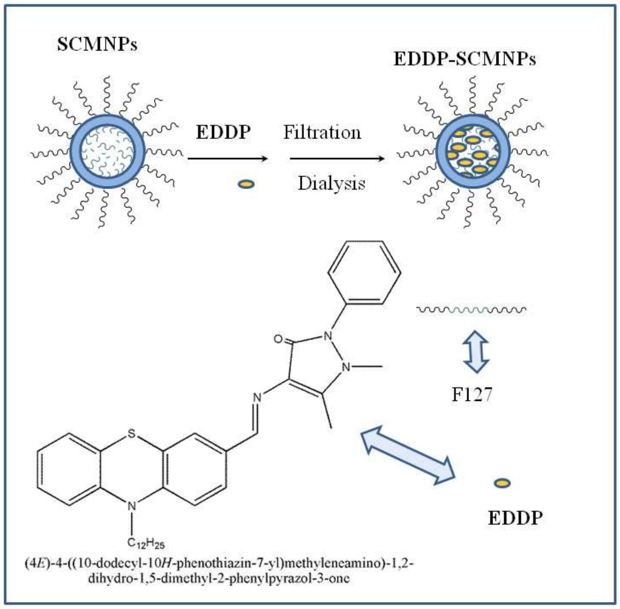

Scheme 1 Synthesis route of EDDP-SCMNPs

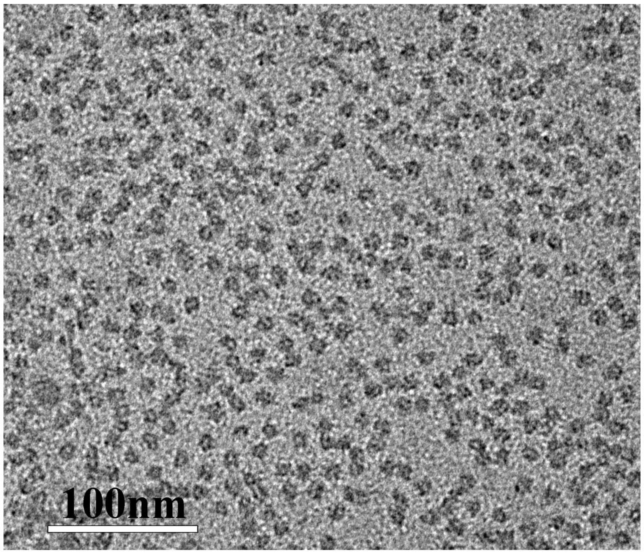

Fig. 1 TEM image of EDDP-SCMNPs (scale bar 100nm)

Fluorescence and absorption of EDDP-SCMNPs

We have added acetonitrile to the free EDDP aqueous solution (acetonitrile: water = 3:7) for improving the solubility of EDDP. The influence of acetonitrile on the fluorescence property of EDDP is minor, which only causes slightly shift of fluorescence emission band of EDDP. Fig. 2 shows the fluorescence emission spectra of free EDDP and EDDP-SCMNPs. The emission spectrum of EDDP-SCMNPs was broader than that of free EDDP. Compared with fluorescence emission of free EDDP (524nm), the fluorescence emission peak of EDDP-SCMNPs located at 527nm which has a slight red-shift of 3 nm. The red-shift in the emission of the EDDP-SCMNPs is attributed to the increased inner molecular interactions as a result of the encapsulation of $C_{12}H_{25}$ chains of EDDP inside the core of SCMNPs. Such shift and broaden behavior was consistent with previous report by Wang *et al.*, which indicates rapid energy transfer via π-conjugated structure occurred in micellar core.[49]

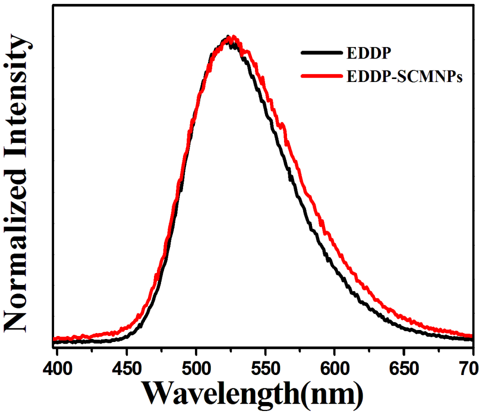

Fig. 2 Fluorescence emission (excitation 377nm) spectra of free EDDP in (black line) and EDDP-SCMNPs (red line)

To elaborate EDDP intermolecular interactions in ground state, we investigate absorption spectra of both EDDP-SCMNPs and free EDDP. As is shown in Fig. S3, the absorption of EDDP-SCMNPs has a red-shift of 4nm and is broader than that of free EDDP. The UV spectra changing and broadening is attributed to the environment of EDDP in the core of nanoparticles. [49]

Considering the change of fluorescence steady-spectra and absorption spectra resulted from EDDP intermolecular interactions between ground state and excited state in hydrophobic core, we anticipated that, based on difference of UV spectra between EDDP-SCMNPs and free EDDP, EDDP-SCMNPs facilitate electron transfer in ground state. On the other hand, the encapsulated EDDP molecules remain the fluorescence property of EDDP.

Selectively detection of Fe^{3+} in water

To examine the feasibility of free EDDP as a chemodosimeter for Fe^{3+} and Fe^{2+}, we first investigated its absorption character in the absence and presence of Fe^{3+} or Fe^{2+}. As is shown in Fig. S4, while upon the addition of Fe^{3+} (2.6 ppm) to free EDDP (1.72×10^{-4} M) solution, EDDP absorption band centred at 320 nm disappeared. Correspondingly, a new peak located at 284 nm was observed. While the addition of Fe^{2+} (2.6 ppm) does not change the absorption of EDDP. However, an increasing amount of Fe^{2+} (17 ppm) causes a decrease absorption band at 320 nm and a new peak at 284nm. The Fe^{2+} and Fe^{3+} decreased absorbance of free EDDP (Fig. S4), which maybe ascribe to the formation of complex during sensing process.[50] The influences of Fe^{3+} and Fe^{2+} on the absorption spectra of free EDDP exhibit the same trend.

Fig.3 (A) shows fluorescence emission of free EDDP at 523nm in the absence of Fe^{3+}. After the addition of Fe^{3+} (up to 2.2 ppm) into the free EDDP solution, an intensity quenching and a red-shift of 45nm (from 523 nm to 568 nm) were observed in fluorescence emission spectra. However, as is shown in Fig.3 (B), 2.2 ppm of Fe^{2+} would not cause EDDP quenching. EDDP fluorescence quenched slightly with a red shift of 3 nm by high concentration of Fe^{2+} (17 ppm). The quenching effect for both Fe^{3+} and Fe^{2+} could be ascribed to metal-promoted hydrolysis.[12-14] This result was further supported by ^1H NMR spectroscopy and MS analysis (Fig. S5 and Fig. S6).

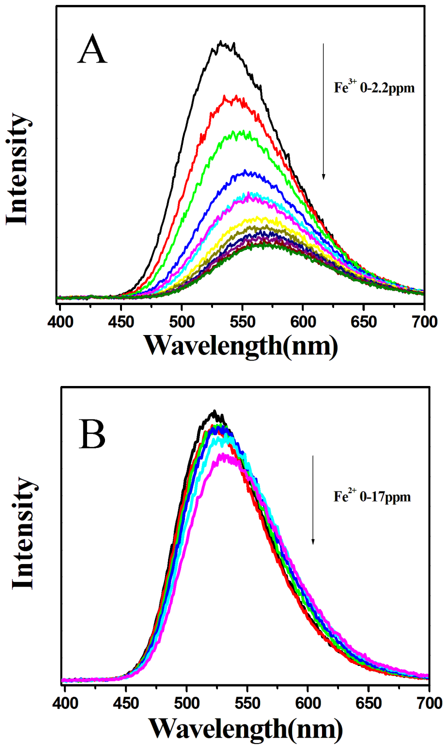

Fig. 3 Fluorescence emission spectra of EDDP added with an increasingly amount of **(A)** Fe^{3+} and **(B)** Fe^{2+}

Based on the above results obtained in free EDDP system, our effort has been made to encapsulate EDDP in the core of SCMNPs for inhibition of metal-promoted hydrolysis quenching, thus constructing electron transfer-based Fe^{3+} selectively detection system.

As is shown in Fig. S7, the presence and absence of Fe^{3+} (32 ppm) in normalized absorption of EDDP-SCMNPs showed a slight difference. The weak absorption band of 380 nm disappeared and a new peak was observed at 272nm by adding Fe^{3+} to EDDP-SCMNPs. This result indicated that the influence of Fe^{3+} induced electronic change of EDDP-SCMNPs in ground state. The influence of Fe^{2+} (32 ppm) did not induce obvious change of EDDP-SCMNPs absorption, which shows almost no electronic interaction between Fe^{2+} and EDDP-SCMNPs in ground state.

Fig. 4(A) shows fluorescence spectra of EDDP-SCMNPs quenched regularly by adding an increasing amount of Fe^{3+} (up to 160 ppm). EDDP-SCMNPs featured high water-solubility and displayed strong fluorescence at 527 nm. Fe^{3+} resulted in the sharply quenching but no shift of EDDP-SCMNPs emission. With the amount of Fe^{3+} increasing in the system, the emission intensity of EDDP-SCMNPs gradually decreased without any change in the shape of emission band. Thus, the mechanism of Fe^{3+} effect on EDDP-SCMNPs is significantly different from that on free EDDP. The maintenance of the shape and wavelength in fluorescence emission spectra implies that Fe^{3+} does not destroy the structure of EDDP in the core of SCMNPs. As we inferred previously, the core of SCMNPs was composed of PPO chains which is hydrophobic and cannot afford the entry of Fe^{3+}. Thus, the hydrolysis reaction of schiff base has not been observed in EDDP-SCMNPs sensing system. TEM images also showed that Fe^{3+} did not influence EDDP-SCMNPs morphology, which suggested that the fluorescence quenching was not caused by the damage or collapse of the nanoparticles. It is impossible for Fe^{3+} to enter into hydrophobic core of EDDP-SCMNPs, which indicates that the emission quenching is not caused by metal-promoted hydrolysis. Moreover, Fe^{3+} is likely to adsorb on the surface of EDDP-SCMNPs shell which was constructed by negatively charged silica with PEO chains extending in aqueous media.

As is shown in Fig. 4(B), the fluorescence emission of EDDP-SCMNPs was almost no change by Fe^{2+} (to 170 ppm), which suggested almost no influence of Fe^{2+} was detected in the steady fluorescence spectra. When an increasingly amount of Fe^{2+} (up to 340 to 1700 ppm) was added, almost no obvious decrease of fluorescence intensity was found in EDDP-SCMNPs fluorescence (Fig. S8). This result indicated that the hydrolysis did not occur in EDDP-SCMNPs sensing system even the concentration of Fe^{2+} is rather high.

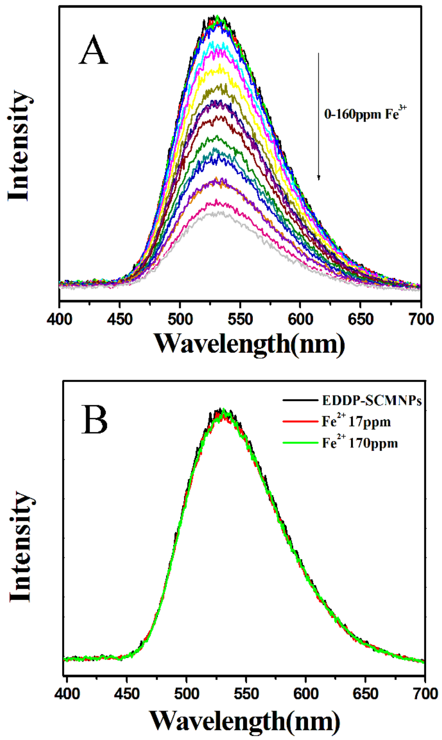

Fig. 4 Fluorescence emission spectra of EDDP-SCMNPs (EDDP 1×10^{-5} M) added with a increasingly amount of **(A)** Fe^{3+} and **(B)** Fe^{2+}

We confirmed the above result by investigating the fluorescence quenching effect of Fe^{3+} and EDTA mixture on free EDDP and EDDP-SCMNPs (Fig. S9). We found that fluorescence emission of free EDDP was quenched by Fe^{3+} (4 ppm), while the emission was almost not quenched by the mixture of Fe^{3+} and EDTA (4 ppm, molar ratio = 1). For the EDDP-SCMNPs system, both 40 ppm of Fe^{3+} and the mixture of Fe^{3+} and EDTA (40 ppm, molar ratio = 1) cause a similar obvious decrease of fluorescence emission. Therefore, the mechanism of EDDP-SCMNPs sensing is not the same as free EDDP in solution.

We further explore the influence mechanism of Fe^{3+} on emission and the absorption of EDDP-SCMNPs. As shown in Fig. 5(A), we found that the emission band of the EDDP-SCMNPs added with Fe^{3+} was located at 527 nm, which shows no overlap with the absorption band of 272nm in aqueous solution. Therefore, the fluorescence resonance energy transfer (FRET) would not occur in the mixture of EDDP-SCMNPs and Fe^{3+}. It is most possible that the quenching of EDDP-SCMNPs by Fe^{3+} should be ascribed to electron transfer mechanism. Because the zeta potential of EDDP-SCMNPs is -10.3mV which is negatively charged, when Fe^{3+} ions are added into the system, the surface of EDDP-SCMNPs would be adsorbed Fe^{3+} onto the silica shell via electrostatic attractions. Therefore, the distance between EDDP in the core and Fe^{3+} on the shell satisfied the distance of electron transfer from EDDP to Fe^{3+}.

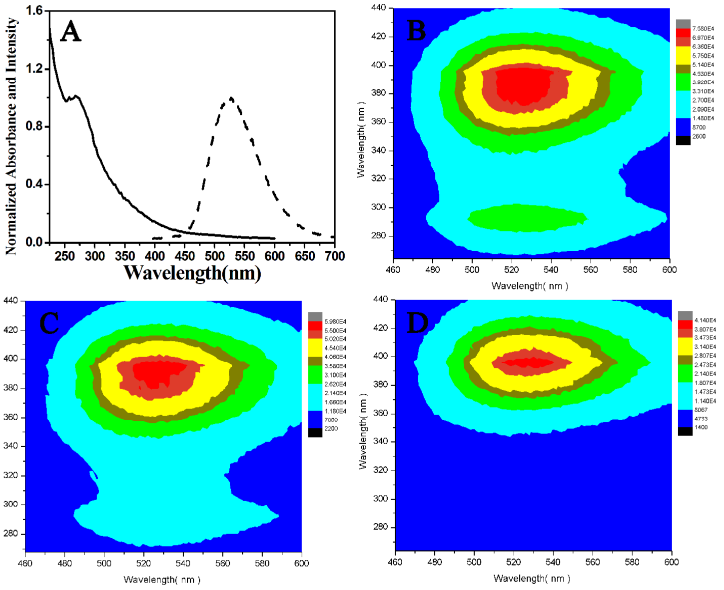

Fig. 5 (A) Normalized absorption spectra (black line) and fluorescence emission spectra (dash line) of EDDP-SCMNPs with Fe^{3+}; 3D fluorescence spectra of (B) EDDP-SCMNPs, (C) EDDP-SCMNPs with 17ppm of Fe^{3+} and (D) EDDP-SCMNPs with 170ppm of Fe^{3+}

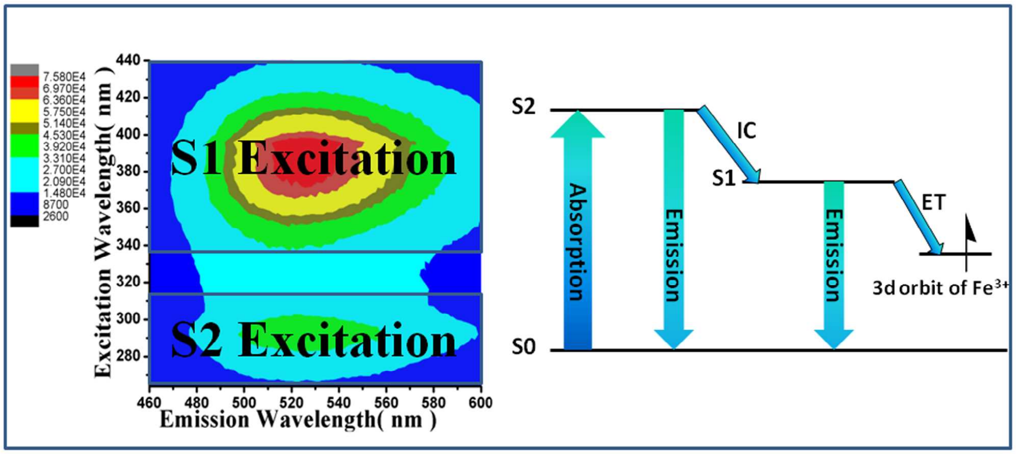

Scheme 2 The vibration of excited state and the energy level of ET explanation

More result of ET process have been given by 3D fluorescence spectroscopy, as is shown in Fig. 5 (B-D), the intensity of fluorescence is plotted as a function of both the excitation and emission wavelengths. The observation of two different excitation bands of (EX/EM: 290/524 nm) and (EX/EM: 380/524nm) for EDDP-SCMNPs (Fig. 5(B)) is either due to two different ground state species or one single species that undergoes an excited state reaction such as electronic transfer or tautomerisation.[51, 52] As is shown in Fig. S7, we found that the 3D spectroscopy of free EDDP exhibit a similar shape compare to that of EDDP-SCMNPs in the emission. Moreover, the EX: 280-350 nm of free EDDP (Fig. S10) and EDDP-SCMNPs (Fig. 5 (B)) are both observed. This clearly rules out the similar wavelength excitation bands of 280-350 nm which may result from twist of EDDP undergoes an excited state reaction due to encapsulation process. When a low concentration of Fe^{3+} (17 ppm) added into EDDP-SCMNPs sensing system, a quenching of excitation band from 280nm to 300nm was detected (Fig. 5(C)). With Fe^{3+} increase, a sharp quenching of spectra was found (EX: 270nm-350nm and EM: 480nm-590nm), which result in only one center at EX/EM: 380/524nm. (See Fig.5D) We believe that the quenching of 3D spectra by Fe^{3+} was attributed to electronic transfer from EDDP in the core to Fe^{3+} attached to the shell. The contour version of the spectrum (Fig.5B) is corresponded to the accompanying generalized Jablonski energy-level diagram[41, 52] (Scheme 2) to display electron transitions available during excitation. The five d half-filled $4s^23d^5$ orbits of Fe^{3+} facilitated the transfer of electrons from the core of EDDP-SCMNPs to 3d orbits of Fe^{3+}. This explanation of quenching mechanism was similar to the literature.[41, 52, 53] Therefore, the two excitation vibration states of EDDP-SCMNPs enable electron transfer from the core of SCMNPs to Fe^{3+}.

Subsequently, the influence of Fe^{2+} on the fluorescence of EDDP-SCMNPs was tested in aqueous solution under the same condition. In the presence of Fe^{2+}, fluorescence emission spectra of EDDP-SCMNPs showed almost no change due to the weak electron-accepting ability of Fe^{2+}. (Fig. 4 (B)). The kinetic curve of Fe^{3+} sensing was tested (Fig. S11). Moreover, EDDP-SCMNPs showed minor sensing ability to other transition metal ions (Fig. 6). The distinctive responses should be resulted from the strong electron-accepting ability of Fe^{3+} which exhibit a more easily capture of electrons.[41]

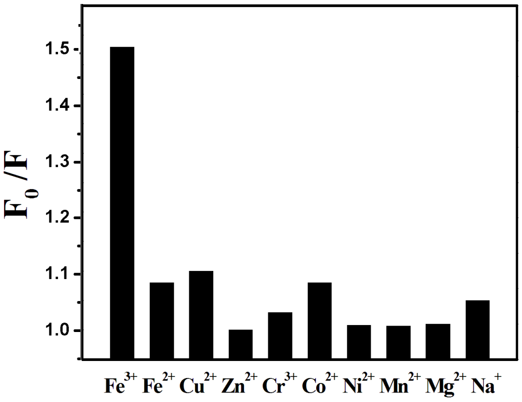

Fig. 6 Selectivity detection of EDDP-SCMNPs sensing system. (All the metal ions are tested at the concentration of 20 ppm)

Thus, a luminescent chemosensor based on EDDP-SCMNPs with highly selective determination of Fe^{3+} has been obtained. We can use H_2O_2 to oxidize Fe^{2+} into Fe^{3+} for the detection of Fe^{2+}.[41] Therefore, Fe^{2+} determination can be achieved via two steps by this luminescent chemosensor EDDP-SCMNPs system.

Conclusion

In summary, we have designed and synthesized an ET-based fluorescence quenching chemosensor using SCMNPs as scaffolds to encapsulate EDDP. The ET process from EDDP in micellar core to Fe^{3+} on the shell was supported using 3D fluorescence spectra and energy-level diagram. Our chemosensor system has two features: (1) The hydrophobic core of EDDP-SCMNPs prevent Fe^{2+}/ Fe^{3+} and water from entering into the core, which inhibited metal-promoted hydrolysis of EDDP. (2) EDDP-SCMNPs favour ET-based highly selective determination of Fe^{3+}, which make a distinction between Fe^{3+} and Fe^{2+} in water. Therefore, the stable, water-soluble and biocompatible EDDP-SCMNPs possess potential application for selective determination of Fe^{3+} in biological systems.

Acknowledgements

This work was supported by the National Natural Science Foundation of China (Nos. 21371067, 21373095 and 21171064)

Notes and references

[a] *State Key Laboratory of Inorganic Synthesis and Preparative Chemistry, College of Chemistry, Jilin University, Changchun 130012, Tel: +86-431-85168602; E-mail: huoqisheng@jlu.edu.cn*
[b] *State Key Laboratory of Supramolecular Structure and Materials, College of Chemistry, Jilin University, Changchun 130012, China. Tel: +86-431-5168484*
[c] *Alan G. MacDiarmid Institute, College of Chemistry, Jilin University, Changchun 130012, China.*

† Electronic Supplementary Information (ESI) available: hydrolysis sensing result tested by NMR and MS, DLS and 3D spectra of EDDP-SCMNPs are shown in supporting information. See DOI: 10.1039/b000000x/

1. S. K. Sahoo, D. Sharma, R. K. Bera, G. Crisponi and J. F. Callan, *Chem. Soc. Rev.*, 2012, **41**, 7195-7227.
2. Y. Yang, Q. Zhao, W. Feng and F. Li, *Chem. Rev.*, 2012, **113**, 192-270.
3. J. H. Wang, *Acc. Chem. Res.*, 1970, **3**, 90-97.
4. A. I. Bush, *Curr. Opin. Chem. Biol.*, 2000, **4**, 184-191.
5. P. Aisen, M. Wessling-Resnick and E. A. Leibold, *Curr. Opin. Chem. Biol.*, 1999, **3**, 200-206.
6. T. Gupta and M. E. van der Boom, *J. Am. Chem. Soc.*, 2007, **129**, 12296-12303.
7. P. Wu, Y. Li and X.-P. Yan, *Analytical Chemistry*, 2009, **81**, 6252-6257.
8. P. Li, L. Fang, H. Zhou, W. Zhang, X. Wang, N. Li, H. Zhong and B. Tang, *Chemistry – A European Journal*, 2011, **17**, 10520-10523.
9. N. R. Chereddy, S. Thennarasu and A. B. Mandal, *Dalton Transactions*, 2012, **41**, 11753-11759.
10. S.-P. Wu, Y.-P. Chen and Y.-M. Sung, *Analyst*, 2011, **136**, 1887-1891.
11. J. Han, Z. Zhou, X. Bu, S. Zhu, H. Zhang, H. Sun and B. Yang, *Analyst*, 2013, **138**, 3402-3408.
12. W. Lin, L. Long, L. Yuan, Z. Cao and J. Feng, *Anal. Chim. Acta*, 2009, **634**, 262-266.
13. W. Lin, L. Yuan, J. Feng and X. Cao, *Eur. J. Org. Chem.*, 2008, **2008**, 2689-2692.
14. M. Zhang, Y. Gao, M. Li, M. Yu, F. Li, L. Li, M. Zhu, J. Zhang, T. Yi and C. Huang, *Tetrahedron Lett.*, 2007, **48**, 3709-3712.
15. Q. Meng, W. Su, C. He and C. Duan, *Talanta*, 2012, **97**, 456-461.
16. G. Ozturk, S. Alp and K. Ertekin, *Dyes and Pigments*, 2007, **72**, 150-156.
17. C. M. G. van den Berg, *Anal. Chem.*, 2005, **78**, 156-163.
18. J. E. T. Andersen, *Analyst*, 2005, **130**, 385-390.
19. G. L. Arnold, S. Weyer and A. D. Anbar, *Anal. Chem.*, 2003, **76**, 322-327.
20. M. E. del Castillo Busto, M. Montes-Bayón, E. Blanco-González, J. Meija and A. Sanz-Medel, *Anal. Chem.*, 2005, **77**, 5615-5621.
21. K. Pomazal, C. Prohaska, I. Steffan, G. Reich and J. F. K. Huber, *Analyst*, 1999, **124**, 657-663.

22. A. P. de Silva, H. Q. N. Gunaratne, T. Gunnlaugsson, A. J. M. Huxley, C. P. McCoy, J. T. Rademacher and T. E. Rice, *Chem. Rev.*, 1997, **97**, 1515-1566.
23. B. Wang, J. Hai, Z. Liu, Q. Wang, Z. Yang and S. Sun, *Angew. Chem. Int. Ed.*, 2010, **49**, 4576-4579.
24. T. Zhang, H. Fan, G. Liu, J. Jiang, J. Zhou and Q. Jin, *Chem. Commun.*, 2008, 5414-5416.
25. J. Du, M. Hu, J. Fan and X. Peng, *Chem. Soc. Rev.*, 2012, **41**, 4511-4535.
26. M. H. Lee, T. V. Giap, S. H. Kim, Y. H. Lee, C. Kang and J. S. Kim, *Chem. Commun.*, 2010, **46**, 1407-1409.
27. J. P. Sumner and R. Kopelman, *Analyst*, 2005, **130**, 528-533.
28. E. Rampazzo, S. Bonacchi, D. Genovese, R. Juris, M. Sgarzi, M. Montalti, L. Prodi, N. Zaccheroni, G. Tomaselli, S. Gentile, C. Satriano and E. Rizzarelli, *Chemistry – A European Journal*, 2011, **17**, 13429-13432.
29. V. K. Bhardwaj, P. Saluja, G. Hundal, M. S. Hundal, N. Singh and D. O. Jang, *Tetrahedron*, 2013, **69**, 1606-1610.
30. K. Kaur, R. Saini, A. Kumar, V. Luxami, N. Kaur, P. Singh and S. Kumar, *Coord. Chem. Rev.*, 2012, **256**, 1992-2028.
31. H. J. Jung, N. Singh and D. O. Jang, *Tetrahedron Lett.*, 2008, **49**, 2960-2964.
32. M. Montalti, E. Rampazzo, N. Zaccheroni and L. Prodi, *New Journal of Chemistry*, 2013, **37**, 28-34.
33. V. Luxami and S. Kumar, *RSC Advances*, 2012, **2**, 8734-8740.
34. S. Palantavida, N. V. Guz and I. Sokolov, *Particle & Particle Systems Characterization*, 2013, **30**, 804-811.
35. I. Sokolov, S. Palantavida, N. V. Guz and C. D. Woodworth, *Abstracts of Papers of the American Chemical Society*, 2012, **243**.
36. V. Kalaparthi, S. Palantavida and I. Sokolov, *Abstracts of Papers of the American Chemical Society*, 2012, **244**.
37. L. Wang and W. H. Tan, *Nano Lett.*, 2006, **6**, 84-88.
38. R. P. Bagwe, C. Yang, L. R. Hilliard and W. Tan, *Langmuir*, 2004, **20**, 8336-8342.
39. S. Bonacchi, D. Genovese, R. Juris, M. Montalti, L. Prodi, E. Rampazzo and N. Zaccheroni, *Angew. Chem. Int. Ed.*, 2011, **50**, 4056-4066.
40. W. Tan, K. Wang, X. He, X. J. Zhao, T. Drake, L. Wang and R. P. Bagwe, *Med. Res. Rev.*, 2004, **24**, 621-638.
41. Q. Mei, C. Jiang, G. Guan, K. Zhang, B. Liu, R. Liu and Z. Zhang, *Chem. Commun.*, 2012, **48**, 7468-7470.
42. W. T. Huang, W. Y. Xie, Y. Shi, H. Q. Luo and N. B. Li, *Journal of Materials Chemistry*, 2012, **22**, 1477-1481.
43. T. Hirayama, K. Okuda and H. Nagasawa, *Chemical Science*, 2013, **4**, 1250-1256.
44. D. Genovese, S. Bonacchi, R. Juris, M. Montalti, L. Prodi, E. Rampazzo and N. Zaccheroni, *Angew. Chem. Int. Ed.*, 2013, **52**, 5965-5968.
45. Q. Huo, J. Liu, L.-Q. Wang, Y. Jiang, T. N. Lambert and E. Fang, *J. Am. Chem. Soc.*, 2006, **128**, 6447-6453.
46. F. Gai, T. Zhou, L. Zhang, X. Li, W. Hou, X. Yang, Y. Li, X. Zhao, D. Xu, Y. Liu and Q. Huo, *Nanoscale*, 2012, **4**, 6041-6049.
47. L. Bian, G. Sun, Y. Sun and W. Tang, *J. Phys. Org. Chem.*, 2012, **25**, 1112-1118.
48. Y.-M. Lam, N. Grigorieff and G. Goldbeck-Wood, *PCCP*, 1999, **1**, 3331-3334.
49. H. Tan, Y. Zhang, M. Wang, Z. Zhang, X. Zhang, A. M. Yong, S. Y. Wong, A. Y.-c. Chang, Z.-K. Chen, X. Li, M. Choolani and J. Wang, *Biomaterials*, 2012, **33**, 237-246.
50. L. Wang, L. Yang and D. Cao, *Sensors Actuators B: Chem. DOI: 10.1016/j.snb.2014.06.052*
51. G. C. Smith and J. F. Sinski, *Appl. Spectrosc.*, 1999, **53**, 1459-1469.
52. V. Thiagarajan, C. Selvaraju, E. J. P. Malar and P. Ramamurthy, *ChemPhysChem*, 2004, **5**, 1200-1209.
53. G. C. Smith and J. F. Sinski, *Appl. Spectrosc.*, 1999, **53**, 1459-1469.

TOC

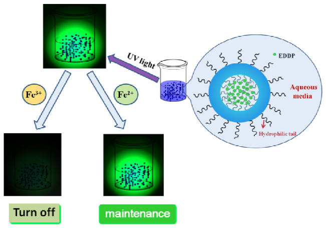

This work demonstrated that the design and synthesis of an ET-based fluorescence quenching chemosensor using silica cross-linked micellar nanoaparticles as scaffolds to encapsulate EDDP for highly selective determination of Fe^{3+} in aqueous media.